Immobilization of *Aspergillus sp.* laccase on hierarchical silica MFI zeolite with embedded macropores

*Davide Tocco[1,2,3], Dorothea Wisser[1], Marcus Fischer[1], Wilhelm Schwieger [1], Andrea Salis[2,3], Martin Hartmann[1,]**

[1] Erlangen Center for Interface Research and Catalysis (ECRC), FAU Erlangen-Nürnberg, Egerlandstr. 3, 91058 Erlangen, Germany.
[2] Department of Chemical and Geological Sciences, University of Cagliari, Cittadella Universitaria, SS 554 bivio Sestu, 09042, Monserrato (CA) (Italy).
[3] Consorzio Interuniversitario per lo Sviluppo dei Sistemi a Grande Interfase (CSGI), via della Lastruccia 3, 50019, Sesto Fiorentino (FI), Italy.

*Corresponding author. E-mail: martin.hartmann@fau.de; ORCID ID: 0000-0003-1156-6264

Statistical summary
4641 words
7 Figures
1 Table

Abstract

Laccase from *Aspergillus sp*. (LC) was immobilized on functionalized silica hierarchical (microporous-macroporous) MFI zeolite (ZMFI). The obtained immobilized biocatalyst (LC@ZMFI) was characterized by X-ray diffraction (XRD), scanning electron microscopy (SEM), Fourier transform infrared spectroscopy (ATR-FTIR), N_2 adsorption/desorption isotherms, solid-state NMR spectroscopy and thermogravimetric analysis (TGA) confirming the chemical anchoring of the enzyme to the zeolitic support. The optimal pH, kinetic parameters (K_M and V_{max}), specific activity, as well as both storage and operational stability of LC@ZMFI were determined. The LC@ZMFI K_M and V_{max} values amount to 10.3 µM and 0.74 µmol · mg^{-1} min^{-1}, respectively. The dependence of specific activity on the pH for free and immobilized LC was investigated in the pH range of 2 to 7, The highest specific activity was obtained at pH = 3 for both free LC and LC@ZMFI. LC@ZMFI retained up to 50% and 30% of its original activity after storage of 21 and 30 days, respectively. Immobilization of laccase on hierarchical silica MFI zeolite allows to carry out the reaction under acidic pH values without affecting the support structure.

KEYWORDS: Laccase; zeolite; hierarchical porous materials; enzyme immobilization; enzyme activity.

Graphical abstract

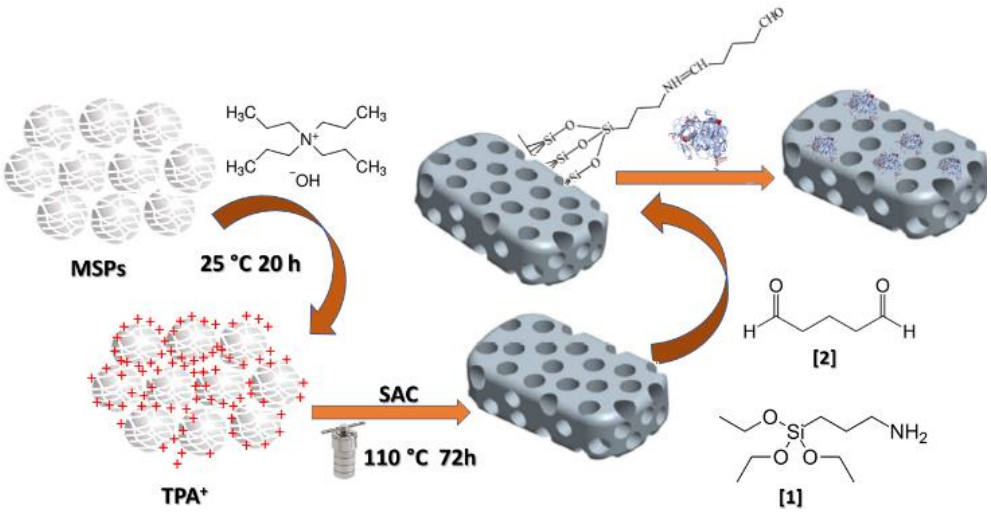

1. Introduction

The demand of enzymes involved in industrial processes, such as food processing,[1] leather treatment,[2] textile,[3] wastewater treatment,[4] pharmaceutical chemistry,[5] biofuels production,[6,7] bioremediation,[8] is continuously growing. The current global enzyme market is valued at $5.5 billion and by 2023 it is predicted to reach $7.0 billion.[9] Laccases (E.C. 1.10.3.2, p-diphenol: dioxygen oxidoreductase) are active toward a wide range of substrates. To date, laccases (LCs) have been investigated for several applications, such as bleaching of denim and paper,[10] removal of toxicants released during combustion processes,[11] decolorization,[12] removal of phenols from wastewaters,[13] and biomass delignification.[14] LCs are constituted by a polypeptide chain containing about 500 amino acids residues and linked to saccharide molecules. The amino acids residues are arranged in three domains.[15,16] One mononuclear copper site containing a type I Cu is located at the T1 site, where the reducing substrate binds, and it is responsible for the characteristic colour of the enzyme in the oxidized state Cu^{2+}.[15] The trinuclear copper site contains one type II Cu and two type III Cu. Substrate oxidation at the mononuclear site generates electrons that are transferred to the trinuclear site where O_2 is reduced to H_2O.[15] Copper species can be classified according to their spectroscopic behaviour. The T1 copper has a strong absorption around 600 nm, while the T2 copper shows a weak absorption in the visible region but is EPR-active. The two coppers of the T3 site display an absorption band at about 330 nm. They are EPR silent due to an antiferromagnetic coupling mediated by a bridging ligand.[16] Their molecular mass commonly ranges between 50 and 140 kDa, but it has been reported to be from 34 to 383 kDa for laccases from *Pleurotus eryngii* and *Podospora anserina*.[7] The LC's isoelectric point is usually around 4.0, even if there are some laccases with alkali isoelectric points.[17] Although LCs present several advantages compared with synthetic catalysts, their use in native form for industrial processes is often hampered by harsh reaction conditions (such as extreme pH values and temperatures), which could result in loss of catalytic activity.[18] Immobilization on solid supports is considered an attractive technology for making enzymes suitable for biotechnological applications.[19] Indeed, immobilized enzymes usually display higher resistance to harsh environmental conditions, allow reusability and may result in improved thermal stability compared to free enzymes.[20]

The enzymatic activity and stability depend on the choice of the support as well as the type (e.g. physical or covalent) of enzyme immobilization.[19,21–23] Nowadays, a wide range of supports, e.g. mesoporous silica,[13,19,24,25], xerogels,[26] magnetic nanomaterials,[27] agarose,[28] nanofibrous polymers[29] and metal organic frameworks[30–34] have been explored as enzyme carriers. Among the several materials reported in the literature, due to their high surface area,[35] and their well-defined pore systems, zeolites could in principle be suitable carriers for enzyme immobilization.[36] However, most zeolites are microporous materials (pore size < 2 nm) and, thus, not suitable for enzyme immobilization. In the last 15 years, a new class of materials called hierarchically-ordered zeolites, constituted by a hierarchical pore system (bimodular or multimodular) has received increasing attention. Although the utilization of zeolites as enzyme carriers is limited by their narrow micropores, the synthesis of zeolitic systems with intracrystalline meso- or macropores can overcome this issue allowing to use zeolites as hosts for enzymes or other biomacromolecules.[37–41]. From the synthetic point of view, the introduction of macropores in zeolites is often hampered by several limitations such as the low wettability of the hard templates with zeolite precursors, poor thermal stability of the template under zeolite synthesis conditions, difficulties in controlling the thickness of the zeolitic walls, and the template removal after hydrothermal synthesis. Nevertheless, most of these drawbacks could be avoided using mesoporous silica particles (MSPs) as templates for macropore formation.[37,42] Recently, a three step procedure to obtain a MFI-type zeolite (the MFI topology consists of intersecting straight and sinusoidal channels[43]) with embedded macropores (with a diameter in the range 250 - 500 nm) has been reported by Machoke *et al*.[37] This material is termed ZMFI.

Since LCs from fungi show higher activity and stability under acidic conditions (i.e., pH 3–6). LCs immobilization on stable supports in this pH range such as silica material could be significant for their stabilization and activity performance. In this work, laccase from *Aspergillus sp.* was immobilized on hierarchical micro/macroporous silica MFI zeolite (acid stable material) to obtain LC@ZMFI biocatalyst with a high immobilization efficiency of 79.4 % and a loading of 9.72 mg g^{-1} compared to other works reported in the literature.[44,45] For example Qiu et al. immobilized laccase from *Aspergillus oryzae* on

mesoporous silica obtaining an immobilization efficiency of 43.6 %.[46] The immobilization of the laccase was carried out post-synthetically. The immobilized biocatalyst was characterized employing XRD, SEM, TGA FTIR, N_2 adsorption/desorption isotherms, solid-state Magic Angle Spinning (MAS) NMR spectroscopy and electron spin resonance (ESR) spectroscopy. The free LC, and LC@ZMFI biocatalysts were also characterized in terms of specific activity, kinetics (K_M and V_{max}) and (storage and operational) stability. A V_{max} of 64.7 μmol · mg^{-1} min^{-1} and 0.74 μmol · mg^{-1} min^{-1} and a K_M of 11.2 μM and 10.3 μM were obtained at pH 3 for both free LC and LC@ZMFI, respectively. LC@ZMFI retained up to 50% and 30% of its original activity after storage of 21 and 30 days, respectively.

2. Materials and Methods

2.1 Chemicals

Laccase from *Aspergillus sp* (activity of ≥ 1000 LAMU g^{-1})*;* 2,2'-azinobis-(3-ethylbenzothiazoline-6-sulfonate) diammonium salt (≥ 98%) (ABTS); sodium hydroxide, NaOH; sodium phosphate, monobasic NaH_2PO_4 (99%); sodium phosphate dibasic, Na_2HPO_4 (99%); Bradford reagent; HCl (37%); acetic acid (99%); sodium acetate (anhydrous) (≥ 99.0%); citric acid (≥ 99.5%);(3-Aminopropyl) triethoxysilane (APTES) (99.0%); glutaraldehyde (50% solution in water); cetyltrimethylammonium bromide (CTAB) (98 %); ethanol (96% technical grade) were purchased from Sigma-Aldrich (Germany).TPAOH solution (40 wt% technical grade, from Clariant (Germany). Tetraethyl orthosilicate (TEOS, 98 %) from Alfa Aesar. All reagents were used as received without further purification. Deionized water was used to prepare all aqueous solutions.

2.2 Synthesis of MFI-Type zeolite

The synthesis MFI-Type zeolite was carried out following the procedure reported by Machoke *et al.*[37] Briefly, in each crucible 250 mg of mesoporous silica particles (MSPs) and 340 mg of TPAOH solution (40 wt% technical grade) were mixed and dried at RT (20 °C) for 20h. First, the MSPs have been weighted and then TPAOH has been added dropwise. Afterwards, the mix of reaction was gently mixed with a spatula and transferred into a Teflon-lined stainless-steel autoclave (45 mL) filled with 24 mL of

deionized water. Thereafter, the autoclave was closed and kept in an oven at 383 K for 72h. The white powder was recovered by filtration, washed with deionized water, and dried overnight at 348 K. Finally, the TPA^+ was removed at 823 K for 4 h under air flow.

2.3 Immobilization of laccase on zeolite Type MFI

The immobilization of LC on ZMFI occurred via post-synthetic treatment according to Salis *et al.*[13] Briefly, 125 mg of zeolite type MFI (ZMFI) was added to 3.75 mL of dry toluene, then 125 µL of 3-aminopropyltrimethoxysilane (APTS) was added to the suspension. The mixture was heated under reflux for 15 h. The zeolite-APTS was collected by filtration, washed with acetone, and dried overnight at room temperature under vacuum. Glutaraldehyde-activated (ZMFI-NH=CH) was prepared by soaking 125 mg ZMFI-NH_2 in a mixture of 100 µL 50% aqueous glutaraldehyde and 2.75mL 0.1M phosphate buffer solution (pH = 7.5) for 1 h. The carrier was washed twice with 5 mL of the same buffer for 30 min under stirring, centrifuged and the washing liquors removed. The wet solid was immediately used for laccase immobilization. Finally, the LC immobilization was carried out mixing a in sodium phosphate buffer (100 mM and pH 8.0) with the modified zeolite. the result suspension was stirred for 2 h. The obtained solid (LC@ZMFI) was recovered by centrifugation at 4000 rpm for 4 min, washed 3 times with deionised water and dried at room temperature.

2.4 Characterization of ZMFI and LC@ZMFI samples

Thermogravimetric analysis (TGA) was carried out by means of a TA instruments TGA 2950 in a temperature range from 25 °C to 700°C and a heating ramp of 5 °C min^{-1}, under synthetic air flow (flow rate = 40 mL min^{-1}). Scanning electron microscopy (SEM) analysis was performed by using a Carl-Zeiss Gemini Ultra 55 microscope with an acceleration voltage of 1 kV. Attenuated total reflectance Fourier transform infrared (ATR-FTIR) spectra were recorded using a Jasco FT/IR 4100 equipped with a PIKE GladiATR accessory with a single reflection diamond prism over the wavelength range, 4000 to 500 cm^{-1}. N_2 adsorption/desorption isotherms were recorded at 77 K using an ASAP 2010 (Micromeritics). Samples were firstly degassed under vacuum for 24 h at 80°C. The Brunauer–Emmett–Teller (BET)[47] and the Barret–Joyner–Halenda (BJH) [48] methods were used to calculate the specific surface area, the

pore volume, and the pore size distribution. A Panalytical X'Pert PRO diffractometer with an X'Celerator line detector was used for X-ray diffraction (XRD) experiments with Cu Kα radiation. The data were collected with a 2θ step size of 0.013 ° from 2 ° to 80 ° and an accumulation time of 10.16 s. A Jasco V-650 UV-Vis spectrophotometer was used for enzymatic activity tests.

Solid-state NMR spectra were recorded on a 500 MHz (11.7 T) wide-bore Agilent DD2 spectrometer in a 3.2 mm zirconia rotor. ^{29}Si HPDEC spectra were acquired at 10 kHz MAS rate, by applying a □/2 pulse of 3.5 μs, followed by 86 kHz spinal-64 ^{1}H decoupling. 1200 scans were recorded with a recycle delay of 150 s. ^{13}C CP MAS NMR spectra were acquired at 15 kHz MAS rate. ^{1}H 2.5 □s pulse on ^{1}H was followed by a linear ramp from 41 to 54 kHz, while keeping the ^{13}C RF at 53 kHz. 86 kHz spinal-64 ^{1}H decoupling was applied during acquisition. 25000-33000 scans were averaged with a recycle delay of 2.5 s.

EPR spectra were measured at 100 K on a Bruker EMXmicro at a MW frequency of 9.44 GHz. 5 scans were accumulated at a MW power of 2.02 mW with an attenuation of 20 dB. Modulation amplitude was set to 9 G at a modulation frequency of 100 kHz.

2.5 Determination of encapsulation efficiency

Protein loading and immobilization efficiency of the immobilized biocatalysts, LC@ZFMI, were obtained by means of the Bradford assay.[31,49] Briefly, the protein content was determined using the Bradford reagent (Bio-Rad) and BSA (bovine serum albumin) as the protein standard (20 mg L^{-1}). The calibration curve was built by preparing a set of BSA solutions in acetate buffer pH 5 100 mM at different concentrations (0.5-20 mg L^{-1}) from dilution of the standard solution. Then, a 0.5 mL aliquot of each solution was mixed to 0.5 mL of Bradford reagent in a glass cuvette. After exactly 10 min the absorbance of the solutions was measured at the wavelength of 595 nm.[50] The protein concentration in the supernatant was evaluated by measuring the absorbance (λ = 595 nm) of a mixture containing 0.5 mL of supernatant and 0.5 mL of Bradford reagent after 10 min of incubation. The amount of immobilized protein is calculated from the difference between the amount used for immobilization and the amount that is in the

supernatant. The immobilization efficiency (IE%) is the percent ratio between the amount of immobilized protein and the amount of protein in the immobilizing solution:

$$IE\% = (1- [P]_f / [P]_0) \cdot 100\%$$

where $[P]_0$ and $[P]_f$ are the initial and the final protein concentrations in the immobilising solution. [31,49]

2.6 Determination of biocatalytic activity

The catalytic activities of LC@ZMFI were quantified by Jasco 650 UV-Vis spectrophotometry, at λ = 420 nm (25 °C). The activity measurement of LC@ZMFI was carried out adding 5 mg of LC@ZMFI in 2.845 mL of 100 mM citrate buffer at pH 3. The reaction started by adding to the mixture a volume of 0.150 mL ABTS 5 mM in a cuvette kept under stirring and at T = 25°C. The blank was measured by mixing 2.845 mL of citrate buffer pH 3 100 mM with 5 mg of LC@ZMFI. The activity test of the ZMFI material was carried out as control experiment to evaluate possible interferences between the material and the enzymatic activity. No activity was detected for LC-free ZMFI. All activity measurements were carried out at least in triplicate. Specific activity (U mg^{-1}) was calculated through the following formula:

$$\text{Specific activity} = \frac{slope \cdot \text{Vcuvette} \cdot 1000 \cdot dilution\ factor}{Venzyme \cdot \varepsilon \text{ABTS+.} \cdot c\ (enzyme)} = \left[\frac{\mu\text{mol}}{mg \cdot min}\right] = \left[\frac{U}{mg}\right]$$

One unit (U) of laccase activity is defined as the amount of enzyme required to convert 1.0 μmol of 2,2'-azinobis-(3-ethylbenzothiazoline-6-sulfonate) diammonium salt (ABTS) to $ABTS^{+\cdot}$ per minute at 25 °C.

3. Results and Discussion

3.1 Samples characterization

The XRD patterns (Figure 1a) exhibit sharp reflections at 2θ = 8°, 9°,14°,15°,16°, 24° and 24.5° characteristic for the MFI topology.[37,51] The LC@ZMFI sample reveals a XRD pattern similar to the ZMFI parent material demonstrating that laccase immobilization did not affect the zeolite structure. The N_2 adsorption/desorption isotherms of ZMFI and LC@ZMFI samples are shown in Figure 1b. Both samples display a type I isotherm, which is characteristic for microporous materials.[52] The ZMFI sample

has a specific surface area (S_{BET}) of 534 m^2 g^{-1} that decreases to 297 m^2 g^{-1} for LC@ZMFI (Table 1). Similarly, the pore volume decreases from 0.27 (ZMFI) to 0.13 cm^3 g^{-1} (LC@ZMFI) suggesting the successful post-synthesis immobilization of laccase on silica MFI zeolite.

Table 1. Textural properties of ZMFI and LC@ZMFI and laccase loading and kinetic parameters of ZMFI and LC@ZMFI

Samples	[a]S_{BET} (m^2 g^{-1})	[b]V_p (cm^3 g^{-1})	IE (%)	L (mg g^{-1})	K_M (µM)	V_{max} (µmol · mg^{-1} min^{-1})
ZMFI	534	0.27	-	-	-	-
LC@ZMFI	297	0.13	79.4	9.72	10.3	0.74
Free LC	-	-	-	-	11.2	64.7

[a] Surface area (S_{BET}) obtained from N_2 adsorption/desorption isotherms; [b] Pore volume (V_p)

Thermogravimetric analysis (Figure 1c) confirms the high stability of MFI zeolite in the temperature range between 100 °C and 500 °C, where a negligible mass loss of 2 % was observed. Similarly, no appreciable mass loss at T > 500°C is observed (data not shown). LC@ZMFI shows a mass loss of 4.3% and 4.5% in the ranges 100°C – 220°C and 220°C – 445°C, respectively. At these temperatures, the observed mass loss is likely due to the decomposition of organic molecules and of the immobilized enzyme. Although two clear distinct mass loss steps in those temperature ranges are observed, it is difficult to discriminate which one is ascribable to enzyme mass loss with absolute certainty. Finally, above 445°C, no mass loss for both ZMFI and LC@ZMFI samples is observed. Protein loading (L) of LC@ZMFI sample, quantified by means of the Bradford assay, is 9.72 mg g^{-1} (Table 1) while the immobilization efficiency (IE%, defined as the amount of immobilized protein relative to the total protein amount in the solution) is 79.4 %.

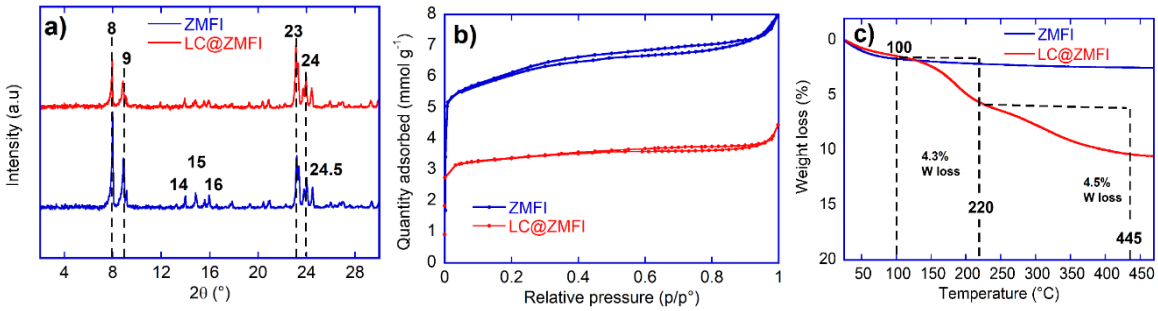

Figure 1. **a)** XRD patterns **b)** N_2 adsorption/desorption isotherms and **c)** thermogravimetric analysis (TGA) of ZMFI and LC@ZMFI in air.

The modification of zeolite MFI (ZMFI) was also monitored employing FT-IR and solid-state NMR spectroscopy. The FT-IR spectrum of the ZMFI (Figure 2) shows a broad band at about 1060 cm^{-1} due to Si-O-Si asymmetric stretching, a band at 960 cm^{-1} due to Si–OH stretching and one at 795 cm^{-1} due to Si–O–Si symmetric stretching. After surface modification with 3-aminopropyl-triethoxysilane (APTES), the band at 960 cm^{-1} disappears and a new band appears at 690 cm^{-1} that is ascribed to N–H bending vibrations. Additional evidence for the zeolite modification are the stretching vibration of C–H bonds at 2870 cm^{-1} , 2900 cm^{-1} and bending vibration of H–C–H bond at 1380 cm^{-1} appear confirming the reaction of free silanols with APTES.[53–55] As a result of laccase immobilization, a band at 1647 cm^{-1} (–C=N– bonds), due to the reaction between the –ZMFI–CHO and laccase appears.

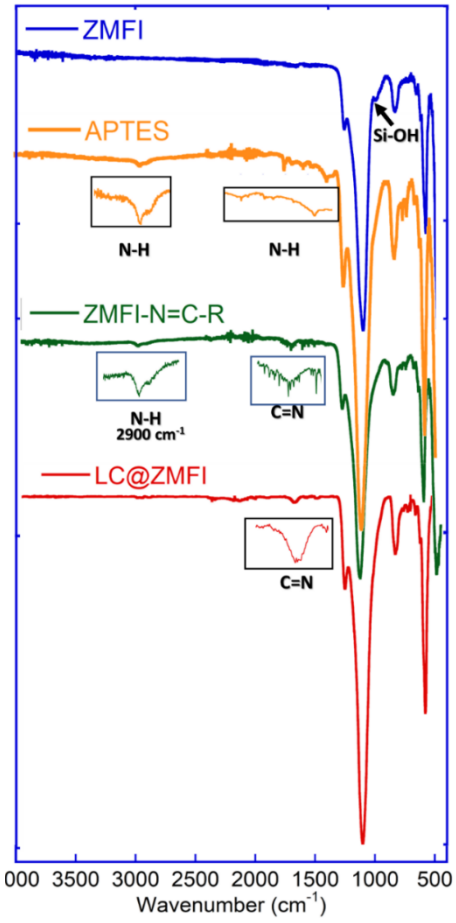

Figure 2. ATR-FT-IR spectrum of parent ZMFI zeolite, the with APTES modified sample and the LC@ZMFI biocatalyst.

^{13}C Cross Polarization (CP) solid-state NMR spectra clearly show the grafting of APTES onto the zeolite, by appearance of resonances at 10, 21, 42 and 58 ppm, characteristic for C_1-C_3 and the amine carbon atom of APTES (Figure 3 a).[56] After modification with glutaraldehyde, additional resonances appear at around

30 ppm, indicative for additional aliphatic groups, and at 62 ppm, assigned to the C=N functionality, but possibly overlapping with unreacted C-NH_2 amine groups from APTES. At 200 ppm, a particularly characteristic resonance for the aldehyde functionality appears. Note that we have not carried out ^{13}C CP MAS NMR on the laccase functionalized ZMFI, as the expected multitude of carbon signals of the enzyme would prohibit further detailed structural analysis. The degree of functionalization was evaluated quantitatively by ^{29}Si direct excitation, high power decoupling (HPDEC) MAS NMR spectra (Figure 3 b). T^2 and T^3 sites corresponding to the surface-grafted species at approx. -50 and -68 ppm are visible, as well as a small amount of hydroxylated silicon sites (Q^3) and non-hydroxylated Si(0Al) sites of the ZMFI framework.[37] Integration of all resonances yields a degree of functionalization of ca. 6 %. Note that this is overall a high degree of functionalization, as most silicon sites are buried inside the zeolite and are not accessible for APTES.

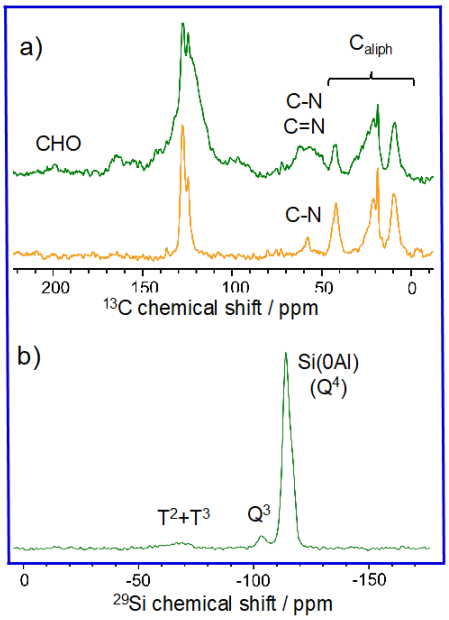

Figure 3. a) ^{13}C CP MAS NMR spectra of ZMFI-NH_2 (yellow) and ZMFI-N=C-R (green). Line broadening: 100 Hz. Signals between 110-130 ppm correspond to toluene from synthesis. **b)** ^{29}Si HPDEC MAS NMR spectrum of ZMFI-N=C-R. Line broadening: 50 Hz.

The sucessful immobilization of LC is furthermore confirmed by ESR spectroscopy (Figure 4), showing that the solid biocatalyst contains LC with no major effect on the close environment of the ESR-active Cu centers of the enzyme.

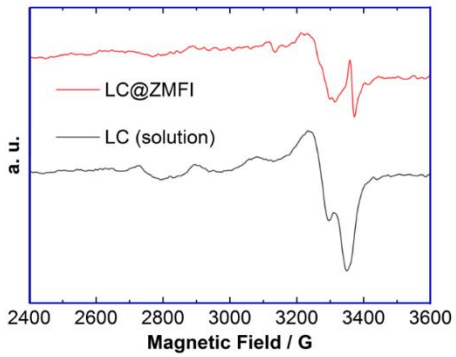

Figure 4. ESR spectra of laccase in solution as supplied and immobilized on ZMFI recorded at 100 K.

Scanning electron microscopy (SEM) images (Figure 5) of ZMFI show particles with the characteristic MFI morphology possesing additional macropores.[37] After laccase immobilization the obtained LC@ZMFI sample retains its morphology in comparison to the parent ZMFI material (Figure 3b).

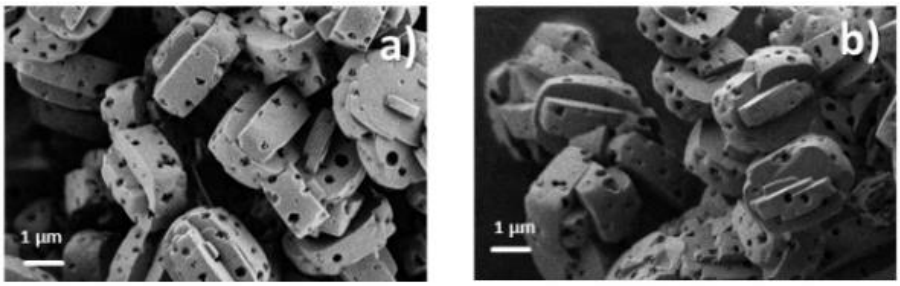

Figure 5. SEM images of **a)** ZMFI **b)** LC@ZMFI.

3.2 Determination of the optimal pH and kinetics for free LC and LC@ZMFI

According to the substrate involved in the reaction mixture, the LCs show different optimal pH values. For example, in the case of phenolic and arylamine substrates involved in the reaction, which entail the release of a proton and an electron, laccases exhibit a bell-shaped pH activity profile with an optimal pH dependent on the laccase and the substrate. This is due to two opposing effects, i) The redox potential difference between the reducing substrate and the T1 Cu (correlating to the electron transfer rate, promoted by higher pH), and ii) The binds of a hydroxide anion to the T2/T3 Cu (which inhibits the activity at a higher pH). It is important to point out that the optimal pH work is related to the nature of LCs. Indeed, fungal laccases such as the LC from *Trametes versicolor* show maximal rates at acidic pH,

whilst bacterial laccases show a clear preference for the basic pH values. The effect of pH on laccase activity was investigated in the pH range of 2 to 7 using 2,2'-azinobis-(3-ethylbenzothiazoline-6-sulfonate) diammonium salt (ABTS) as substrate. The different pH values were obtained by using different buffers, e.g. 100 mM citrate buffer (pH 2 - 4), 100 mM acetate buffer (pH range 5-6) and 100 mM phosphate buffer (pH 7). Both free LC and LC@ZMFI have a similar activity trend, i.e. As the pH was decreased, the activities of both free and immobilized laccase increased. exhibiting a maximum of catalytic activity at pH = 3 (Figure 6a). The activity of LC@ZMFI decreased to almost 50% at pH 5 and to 90% at pH 7 in comparison with the activity at pH 3. This trend is in agreement with what reported by Miller *et al.* for *Aspergillus sp.* laccase immobilized by covalent bonding on nanozeolites.[57] According to these results, the kinetic parameters K_M and V_{max} were determined at pH 3. This is in agreement with e.g. Wang *et al.*[58]

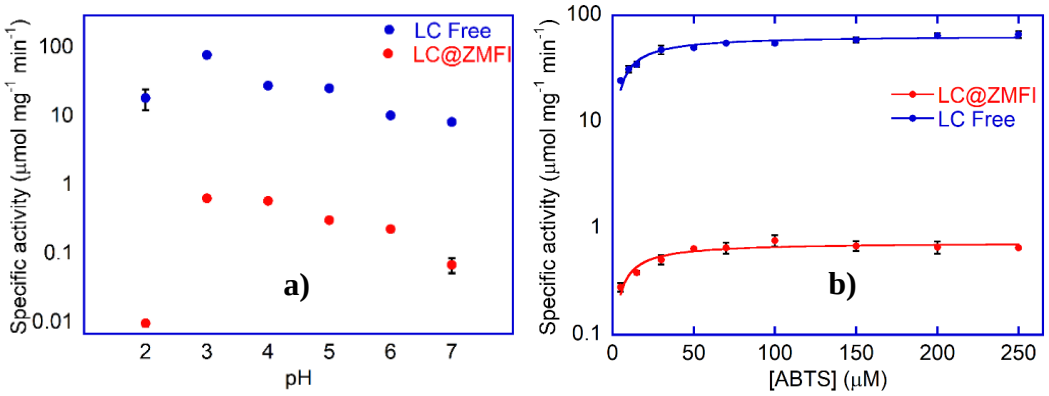

Figure 6. a) Specific activity as a function of pH and **b)** Michaelis-Menten plot for free laccase and LC@ZMFI.

The kinetics of the free and immobilized *Aspergilus sp*. laccase was studied in 0.1 M citrate buffer at pH=3 using 2,2'-azinobis-(3-ethylbenzothiazoline-6-sulfonate) diammonium salt (ABTS) as substrate (Figure 6b). The Michaelis-Menten constant K_M slightly decreases upon immobilization, being 11.2 and 10.3 μM for free LC and LC@ZMFI, respectively (Table 1), suggesting that the immobilization results in a slight increase of enzyme-substrate affinity. This phenomenon could be ascribable to a modification of the enzyme conformation leading to a better accessibility of the substrate to the active sites due to the

immobilization procedure. The V_{max} instead, is strongly affected by immobilization, decreasing from 64.7 (free LC) to 0.74 μmol · mg^{-1} min^{-1} (LC@ZFMI). Such activity decrease has been previously observed for laccases immobilized on other supports.[34] For example, the V_{max} of *Aspergillus sp.* laccase immobilized on Fe-BTC and ZIF-zni metal organic frameworks was 1.32 μmol min^{-1} mg^{-1} and 0.17 μmol min^{-1} mg^{-1} for LC@ZIF-zni and LC@Fe-BTC, respectively.[44] However, a strict comparison of kinetic parameters with the present work cannot be done because the assays were carried out at different pH values. Indeed, Fe-BTC MOF is unstable under acidic conditions, so that LC@Fe-BTC was assayed at pH 5 although the optimal pH for *Aspergillus sp.* laccase is 3. Vera et al. Immobilized laccases from *aspergillus sp,* from *Trametes versicolor* and from *Myceliophthora thermophila* on polymeric microspheres. The kinetic parameter regarding *Aspergillus sp.* and *Trametes versicolor* laccase follows the same trend reported in our work, that is, a decrease of both K_M and V_{max} whilst in the case of *thermophila* laccase their result showed an increase in K_M value and a decrease in V_{max}.[59] Taghizadeh et al. immobilized by physical adsorption a laccase from *Trametes versicolor* on NaY (laccase@NaY) and its modified desilicated and dealuminated forms in order to obtain hierarchical zeolites, laccase@DSY and laccase@DAY respectively. The K_M values were 0.73, 0.26, and 0.31 for the immobilized enzyme and 1.01 ± 0.03mM for the related controls of the free laccase (NaY, DAY, and DSY, respectively).[45] Dos Santos et al. co-immobilized a lipase and a laccase from *Aspergillus sp.* on agarose-based supports. The kinetic parameters regarding of the laccase showed a slight decrease upon immobilization from 0.072 to 0.068 and 0.21 to 0.13 for K_M and V_{max} respectively.[60] Ameri *et al.* reported the immobilization by physical adsorption of laccase from *Trametes versicolor* onto two hierarchical zeolites called HR-Y and HR-Z. They obtained a V_{max} of 1.11 and 1.02 μmol min^{-1} and a K_M of 0.26 and 0.31 mM for HR-Y and HR-Z, respectively.[44] These results demonstrate that the kinetic parameters are affected by the nature of the support and the type (physical, covalent, entrapment, etc.) of immobilization. However, an accurate comparison of our results with those reported in literature is difficult because the specific conditions of the activity assays (e.g. pH) are often different. Moreover, since the reaction rates are proportional to the amount of active enzyme molecules, but the percentage of molecules active immobilized enzymes is

unknown the comparison between kinetics parameter of native laccase to immobilized laccase is often very complicated.[61]

3.3 Storage stability and reuse of LC@ZMFI

Immobilized enzymes are generally subject to a partial or even full inactivation after long storage times.[62] The LC@ZMFI was stored at 4 °C and the residual activity was checked for 30 days. The storage stability of LC@ZMFI retained 52% of its initial activity at the 21st day and about 20% of its initial activity at the 30th day (Figure 7a). Similarly, Zheng *et al.* reported a laccase from *Trametes pubescens* immobilized on chitosan beads showed an activity retention of about 50% after 30 days.[62] The storage stability trend agrees with other works of laccases immobilized on silica materials reported in literature. For example, Hu et al. immobilized a laccase on mesoporous silica particles, their immobilized laccase retained 79.25% and 60.35% of its initial activity after 18 days and 30 days respectively.[63]

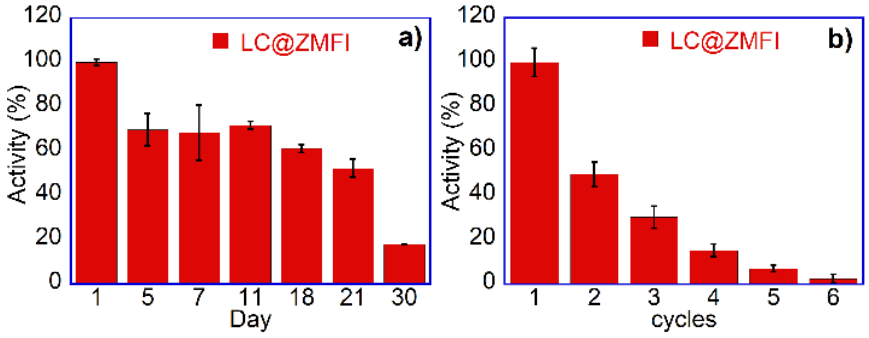

Figure 7. a) Storage stability of LC@ZMFI, activity normalized at 1.12 µmol min^{-1} mg^{-1}. **b)** Reuse of LC@ZMFI, activity normalized at 0.9 µmol min^{-1} mg^{-1}.

Biocatalyst reuse plays a crucial role for reducing the overall costs in industrial applications.[44] Data in Figure 7b show the reuse studies of LC@ZMFI. LC@ZMFI retained 50.5% of its initial activity after the 1st reuse. Thereafter, it retained 30% and 15% of the initial activity at the 2nd and 3rd cycle respectively, which further decreases in the next cycles. The rapid decrease in activity of the LC@ZMFI due to reuse, it might be associated with partial inactivation of enzyme due to the collection procedure. The used biocatalyst was collected by centrifugation and for each reuse cycle of reaction the collected powder was washed with buffer and dried at air atmosphere avoiding keeping washing buffer which would dilute the

mix of reaction. As reported in literature laccase shows extremely high sensitivity to environmental conditions, which means that the stability of laccase is poor under natural conditions. Therefore, the drying process could most likely affect the enzyme activity. However other works reported the rapid decrease in activity for immobilized LCs. For example, Wang et al immobilized a LC in a biochar obtaining a storage stability and reuse comparable with our results.[58] Ameri et al. obtained a immobilized laccase's reusability retention after ten consecutive ABTS oxidation cycles at 5.6%, 6% for LC@NaY and LC@ZSM-5 respectively.[44] The loss of activity due to reuse could be related to the influence of the substrate concentration (ABTS) on the laccase activity. Girelli et al. immobilized a laccase laccase from *Trametes versicolor* on a silica-chitosan hybrid support. The Michaelis-Menten curve of the immobilized enzyme showed substrate inhibition at a high concentration of ABTS.[64] The same phenomenon was observed by Dos Santos et al.[60] It could be possible that ABTS is not totally removed from the biocatalyst after the first reuse cycle leading to an ABTS accumulation that inhibits the laccase activity as a consequence of a rapid LC@ZMFI inactivation.

4. Conclusion

Aspergillus sp. laccase was immobilized onto a hierarchical (microporous-macroporous) MFI zeolite. The structure of MFI zeolite, characterized employing XRD, SEM, TGA, and FTIR, was not affected by LC immobilization. The values of immobilization efficiency and loading were 79.4% and 9.72 mg g^{-1}, respectively. pH strongly affected the activity of both the free LC and LC@ZMFI resulting in a maximum of specific activity at pH 3. The K_M of LC@ZMFI was a bit smaller than that of the free laccase, assayed at pH 3, suggesting a slight increase in enzyme-substrate affinity. V_{max}, instead, was much lower for LC@ZMFI compared with free laccase as a result of a partial inactivation likely due to the immobilization process. The immobilized biocatalyst retained around 70 % of its activity for 11 days, and 50 % after 21 days. It is well known that the enzymatic activity is highly influenced by pH. LCs generally display their optimum activity in the pH range of 3.0–5.5.[65,66] Therefore, the choice of a stable material able to work at the enzymatic optimal pH is crucial. Although the use of MOFs as the enzymatic carriers is widely

described in the literature, recent studies have shown that MOFs are not stable at low pH, [34,67,68] where LCs exhibit maximum activity. The use of the silica hierarchical zeolite allows to carry out the reaction under the optimal pH of laccase avoiding the dissolution of the support. Previous works reported the enzymatic immobilization on different zeolites.[44,69] However, those systems are often affected by mass transfer limitations. To date only few works regard enzymes immobilized on hierarchical zeolites have been reported in literature.[44,45] Further investigation in terms of mass transfer and enzymatic activity at different temperatures will be carried out using this support.

Acknowledgements

DT thanks Deutsche Akademische Austauschdienst (DAAD) and MIUR (PON RI 2014-2020, Azione l.1 "Dottorati Innovativi con Caratterizzazione industriale"- DOT1304455 2) for financing his PhD scholarship and his research period abroad at FAU Erlangen-Nürnberg. AS thanks for financial support from Fondazione di Sardegna (FdS, F72F20000230007), and Regione Autonoma della Sardegna L.R. 7 RASSR79857.

Conflict of interest

The authors declare no conflict of interest.

References

(1) Ottone, C.; Romero, O.; Aburto, C.; Illanes, A.; Wilson, L. Biocatalysis in the Winemaking Industry: Challenges and Opportunities for Immobilized Enzymes. *Compr. Rev. Food Sci. Food Saf.* **2020**, *19* (2), 595–621. https://doi.org/10.1111/1541-4337.12538.

(2) Couto, S. R.; Sanroman, M. A.; Hofer, D.; Gübitz, G. M. Production of Laccase ByTrametes Hirsuta Grown in an Immersion Bioreactor and Its Application in the Docolorization of Dyes from a Leather Factory. *Eng. Life Sci.* **2004**, *4* (3), 233–238. https://doi.org/10.1002/elsc.200420024.

(3) Zerva, A.; Simić, S.; Topakas, E.; Nikodinovic-Runic, J. Applications of Microbial Laccases: Patent Review of the Past Decade (2009–2019). *Catalysts* **2019**, *9* (12), 1023.

https://doi.org/10.3390/catal9121023.

(4) Amari, A.; Alzahrani, F. M.; Alsaiari, N. S.; Katubi, K. M.; Rebah, F. Ben; Tahoon, M. A. Magnetic Metal Organic Framework Immobilized Laccase for Wastewater Decolorization. *Processes* **2021**, *9* (5), 774. https://doi.org/10.3390/pr9050774.

(5) Li, G.; Wang, J.; Reetz, M. T. Biocatalysts for the Pharmaceutical Industry Created by Structure-Guided Directed Evolution of Stereoselective Enzymes. *Bioorg. Med. Chem.* **2018**, *26* (7), 1241–1251. https://doi.org/https://doi.org/10.1016/j.bmc.2017.05.021.

(6) Salis, A.; Monduzzi, M.; Solinas, V. Use of Lipases for the Production of Biodiesel. In *Industrial Enzymes*; Springer Netherlands: Dordrecht, 2007; pp 317–339. https://doi.org/10.1007/1-4020-5377-0_19.

(7) Tocco, D.; Carucci, C.; Monduzzi, M.; Salis, A.; Sanjust, E. Recent Developments in the Delignification and Exploitation of Grass Lignocellulosic Biomass. *ACS Sustain. Chem. Eng.* **2021**, *9* (6), 2412–2432. https://doi.org/10.1021/acssuschemeng.0c07266.

(8) Pitzalis, F.; Monduzzi, M.; Salis, A. A Bienzymatic Biocatalyst Constituted by Glucose Oxidase and Horseradish Peroxidase Immobilized on Ordered Mesoporous Silica. *Microporous Mesoporous Mater.* **2017**, *241*, 145–154. https://doi.org/10.1016/j.micromeso.2016.12.023.

(9) Tarafdar, A.; Sirohi, R.; Gaur, V. K.; Kumar, S.; Sharma, P.; Varjani, S.; Pandey, H. O.; Sindhu, R.; Madhavan, A.; Rajasekharan, R.; Sim, S. J. Engineering Interventions in Enzyme Production: Lab to Industrial Scale. *Bioresour. Technol.* **2021**, *326* (October 2020), 124771. https://doi.org/10.1016/j.biortech.2021.124771.

(10) Unuofin, J. O. Treasure from Dross: Application of Agroindustrial Wastes-Derived Thermo-Halotolerant Laccases in the Simultaneous Bioscouring of Denim Fabric and Decolorization of Dye Bath Effluents. *Ind. Crops Prod.* **2020**, *147* (February), 112251. https://doi.org/10.1016/j.indcrop.2020.112251.

(11) Prasetyo, E. N.; Semlitsch, S.; Nyanhongo, G. S.; Lemmouchi, Y.; Guebitz, G. M. Laccase Oxidation and Removal of Toxicants Released during Combustion Processes. *Chemosphere*

2016, *144*, 652–660. https://doi.org/10.1016/j.chemosphere.2015.07.082.

(12) Zucca, P.; Sanjust, E. Inorganic Materials as Supports for Covalent Enzyme Immobilization: Methods and Mechanisms. *Molecules* **2014**, *19* (9), 14139–14194. https://doi.org/10.3390/molecules190914139.

(13) Salis, A.; Pisano, M.; Monduzzi, M.; Solinas, V.; Sanjust, E. Laccase from Pleurotus Sajor-Caju on Functionalised SBA-15 Mesoporous Silica: Immobilisation and Use for the Oxidation of Phenolic Compounds. *J. Mol. Catal. B Enzym.* **2009**, *58* (1–4), 175–180. https://doi.org/10.1016/j.molcatb.2008.12.008.

(14) Wong, D. W. S. Structure and Action Mechanism of Ligninolytic Enzymes. *Appl. Biochem. Biotechnol.* **2009**, *157* (2), 174–209. https://doi.org/10.1007/s12010-008-8279-z.

(15) Riva, S. Laccases: Blue Enzymes for Green Chemistry. *Trends Biotechnol.* **2006**, *24* (5), 219–226. https://doi.org/10.1016/j.tibtech.2006.03.006.

(16) Piontek, K.; Antorini, M.; Choinowski, T. Crystal Structure of a Laccase from the FungusTrametes Versicolor at 1.90-Å Resolution Containing a Full Complement of Coppers. *J. Biol. Chem.* **2002**, *277* (40), 37663–37669. https://doi.org/10.1074/jbc.M204571200.

(17) Mukhopadhyay, M.; Banerjee, R. Purification and Biochemical Characterization of a Newly Produced Yellow Laccase from Lentinus Squarrosulus MR13. *3 Biotech* **2015**, *5* (3), 227–236. https://doi.org/10.1007/s13205-014-0219-8.

(18) Sheldon, R. A. Metrics of Green Chemistry and Sustainability: Past, Present, and Future. *ACS Sustain. Chem. Eng.* **2018**, *6* (1), 32–48. https://doi.org/10.1021/acssuschemeng.7b03505.

(19) Magner, E. Immobilisation of Enzymes on Mesoporous Silicate Materials. *Chem. Soc. Rev.* **2013**, *42* (15), 6213. https://doi.org/10.1039/c2cs35450k.

(20) Hartmann, M.; Kostrov, X. Immobilization of Enzymes on Porous Silicas – Benefits and Challenges. *Chem. Soc. Rev.* **2013**, *42* (15), 6277. https://doi.org/10.1039/c3cs60021a.

(21) Hanefeld, U.; Gardossi, L.; Magner, E. Understanding Enzyme Immobilisation. *Chem. Soc. Rev.* **2009**, *38* (2), 453–468. https://doi.org/10.1039/B711564B.

(22) Sheldon, R. A.; van Pelt, S. Enzyme Immobilisation in Biocatalysis: Why, What and How. *Chem. Soc. Rev.* **2013**, *42* (15), 6223–6235. https://doi.org/10.1039/c3cs60075k.

(23) Valldeperas, M.; Salis, A.; Barauskas, J.; Tiberg, F.; Arnebrant, T.; Razumas, V.; Monduzzi, M.; Nylander, T. Enzyme Encapsulation in Nanostructured Self-Assembled Structures: Toward Biofunctional Supramolecular Assemblies. *Curr. Opin. Colloid Interface Sci.* **2019**, *44*, 130–142. https://doi.org/10.1016/j.cocis.2019.09.007.

(24) Hanefeld, U.; Cao, L.; Magner, E. Enzyme Immobilisation: Fundamentals and Application. *Chem. Soc. Rev.* **2013**, *42* (15), 6211. https://doi.org/10.1039/c3cs90042h.

(25) Zhou, Z.; Hartmann, M. Progress in Enzyme Immobilization in Ordered Mesoporous Materials and Related Applications. *Chem. Soc. Rev.* **2013**, *42* (9), 3894. https://doi.org/10.1039/c3cs60059a.

(26) Fernandez Caresani, J. R.; Dallegrave, A.; dos Santos, J. H. Z. Amylases Immobilization by Sol–Gel Entrapment: Application for Starch Hydrolysis. *J. Sol-Gel Sci. Technol.* **2020**, *94* (1), 229–240. https://doi.org/10.1007/s10971-019-05136-7.

(27) Wastewater, T.; Siddeeg, S. M.; Tahoon, M. A.; Mnif, W. Iron Oxide / Chitosan Magnetic Nanocomposite Immobilized Manganese Peroxidase For.

(28) Zucca, P.; Fernandez-Lafuente, R.; Sanjust, E. Agarose and Its Derivatives as Supports for Enzyme Immobilization. *Molecules* **2016**, *21* (11), 1577. https://doi.org/10.3390/molecules21111577.

(29) Temoçin, Z.; İnal, M.; Gökgöz, M.; Yiğitoğlu, M. Immobilization of Horseradish Peroxidase on Electrospun Poly(Vinyl Alcohol)–Polyacrylamide Blend Nanofiber Membrane and Its Use in the Conversion of Phenol. *Polym. Bull.* **2018**, *75* (5), 1843–1865. https://doi.org/10.1007/s00289-017-2129-5.

(30) Zhong, L.; Feng, Y.; Wang, G.; Wang, Z.; Bilal, M.; Lv, H.; Jia, S.; Cui, J. Production and Use of Immobilized Lipases in/on Nanomaterials: A Review from the Waste to Biodiesel Production. *Int. J. Biol. Macromol.* **2020**, *152*, 207–222. https://doi.org/10.1016/j.ijbiomac.2020.02.258.

(31) Pitzalis, F.; Carucci, C.; Naseri, M.; Fotouhi, L.; Magner, E.; Salis, A. Lipase Encapsulation onto ZIF-8: A Comparison between Biocatalysts Obtained at Low and High Zinc/2-Methylimidazole Molar Ratio in Aqueous Medium. *ChemCatChem* **2018**, *10* (7), 1578–1585. https://doi.org/10.1002/cctc.201701984.

(32) Carucci, C.; Bruen, L.; Gascón, V.; Paradisi, F.; Magner, E. Significant Enhancement of Structural Stability of the Hyperhalophilic ADH from Haloferax Volcanii via Entrapment on Metal Organic Framework Support. *Langmuir* **2018**, *34* (28), 8274–8280. https://doi.org/10.1021/acs.langmuir.8b01037.

(33) Naseri, M.; Pitzalis, F.; Carucci, C.; Medda, L.; Fotouhi, L.; Magner, E.; Salis, A. Lipase and Laccase Encapsulated on Zeolite Imidazolate Framework: Enzyme Activity and Stability from Voltammetric Measurements. *ChemCatChem* **2018**, *10* (23), 5425.

(34) Tocco, D.; Carucci, C.; Todde, D.; Shortall, K.; Otero, F.; Sanjust, E.; Magner, E.; Salis, A. Enzyme Immobilization on Metal Organic Frameworks: Laccase from Aspergillus Sp. Is Better Adapted to ZIF-Zni Rather than Fe-BTC. *Colloids Surfaces B Biointerfaces* **2021**, *208* (September), 112147. https://doi.org/10.1016/j.colsurfb.2021.112147.

(35) Hartmann, M.; Schwieger, W.; Thommes, M. Hierarchically-Ordered Materials. *Adv. Mater. Interfaces* **2021**, *8* (4), 2100057. https://doi.org/10.1002/admi.202100057.

(36) Corma, A.; Fornes, V.; Rey, F. Delaminated Zeolites: An Efficient Support for Enzymes. *Adv. Mater.* **2002**, *14* (1), 71–74. https://doi.org/10.1002/1521-4095(20020104)14:1<71::AID-ADMA71>3.0.CO;2-W.

(37) Machoke, A. G.; Beltrán, A. M.; Inayat, A.; Winter, B.; Weissenberger, T.; Kruse, N.; Güttel, R.; Spiecker, E.; Schwieger, W. Micro/Macroporous System: MFI-Type Zeolite Crystals with Embedded Macropores. *Adv. Mater.* **2015**, *27* (6), 1066–1070. https://doi.org/10.1002/adma.201404493.

(38) Weissenberger, T.; Machoke, A. G. F.; Reiprich, B.; Schwieger, W. Preparation and Potential Catalytic Applications of Hierarchically Structured Zeolites with Macropores. *Adv. Mater.*

Interfaces **2021**, *8* (4), 2001653. https://doi.org/10.1002/admi.202001653.

(39) Hartmann, M.; Thommes, M.; Schwieger, W. Hierarchically-Ordered Zeolites: A Critical Assessment. *Adv. Mater. Interfaces* **2021**, *8* (4), 2001841. https://doi.org/10.1002/admi.202001841.

(40) Marthala, V. R. R.; Urmoneit, L.; Zhou, Z.; Machoke, A. G. F.; Schmiele, M.; Unruh, T.; Schwieger, W.; Hartmann, M. Boron-Containing MFI-Type Zeolites with a Hierarchical Nanosheet Assembly for Lipase Immobilization. *Dalt. Trans.* **2017**, *46* (13), 4165–4169. https://doi.org/10.1039/C7DT00092H.

(41) Mitchell, S.; Pérez-Ramírez, J. Mesoporous Zeolites as Enzyme Carriers: Synthesis, Characterization, and Application in Biocatalysis. *Catal. Today* **2011**, *168* (1), 28–37. https://doi.org/10.1016/j.cattod.2010.10.058.

(42) Weissenberger, T.; Reiprich, B.; Machoke, A. G. F.; Klühspies, K.; Bauer, J.; Dotzel, R.; Casci, J. L.; Schwieger, W. Hierarchical MFI Type Zeolites with Intracrystalline Macropores: The Effect of the Macropore Size on the Deactivation Behaviour in the MTO Reaction. *Catal. Sci. Technol.* **2019**, *9* (12), 3259–3269. https://doi.org/10.1039/C9CY00368A.

(43) Maesen, T. L. .; Schenk, M.; Vlugt, T. J. .; Smit, B. Differences between MFI- and MEL-Type Zeolites in Paraffin Hydrocracking. *J. Catal.* **2001**, *203* (2), 281–291. https://doi.org/10.1006/jcat.2001.3332.

(44) Ameri, A.; Taghizadeh, T.; Talebian-Kiakalaieh, A.; Forootanfar, H.; Mojtabavi, S.; Jahandar, H.; Tarighi, S.; Faramarzi, M. A. Bio-Removal of Phenol by the Immobilized Laccase on the Fabricated Parent and Hierarchical NaY and ZSM-5 Zeolites. *J. Taiwan Inst. Chem. Eng.* **2021**, *120*, 300–312. https://doi.org/10.1016/j.jtice.2021.03.016.

(45) Taghizadeh, T.; Talebian-Kiakalaieh, A.; Jahandar, H.; Amin, M.; Tarighi, S.; Faramarzi, M. A. Biodegradation of Bisphenol A by the Immobilized Laccase on Some Synthesized and Modified Forms of Zeolite Y. *J. Hazard. Mater.* **2020**, *386* (October 2019), 121950. https://doi.org/10.1016/j.jhazmat.2019.121950.

(46) Qiu, X.; Qin, J.; Xu, M.; Kang, L.; Hu, Y. Organic-Inorganic Nanocomposites Fabricated via Functional Ionic Liquid as the Bridging Agent for Laccase Immobilization and Its Application in 2,4-Dichlorophenol Removal. *Colloids Surfaces B Biointerfaces* **2019**, *179* (March), 260–269. https://doi.org/10.1016/j.colsurfb.2019.04.002.

(47) Brunauer, S.; Emmett, P. H.; Teller, E. Adsorption of Gases in Multimolecular Layers. *J. Am. Chem. Soc.* **1938**, *60* (2), 309–319. https://doi.org/10.1021/ja01269a023.

(48) Barrett, E. P.; Joyner, L. G.; Halenda, P. P. The Determination of Pore Volume and Area Distributions in Porous Substances. I. Computations from Nitrogen Isotherms. *J. Am. Chem. Soc.* **1951**, *73* (1), 373–380. https://doi.org/10.1021/ja01145a126.

(49) Li, H.; Chen, F. Preparation and Quality Evaluation of Coenzyme Q10 Long-Circulating Liposomes. *Saudi J. Biol. Sci.* **2017**, *24* (4), 797–802. https://doi.org/10.1016/j.sjbs.2015.10.025.

(50) Bradford, M. M. A Rapid and Sensitive Method for the Quantitation of Microgram Quantities of Protein Utilizing the Principle of Protein-Dye Binding. *Anal. Biochem.* **1976**, *72* (1), 248–254. https://doi.org/https://doi.org/10.1016/0003-2697(76)90527-3.

(51) Okamoto, M.; Osafune, Y. MFI-Type Zeolite with a Core–Shell Structure with Minimal Defects Synthesized by Crystal Overgrowth of Aluminum-Free MFI-Type Zeolite on Aluminum-Containing Zeolite and Its Catalytic Performance. *Microporous Mesoporous Mater.* **2011**, *143* (2–3), 413–418. https://doi.org/10.1016/j.micromeso.2011.03.032.

(52) Thommes, M.; Kaneko, K.; Neimark, A. V.; Olivier, J. P.; Rodriguez-Reinoso, F.; Rouquerol, J.; Sing, K. S. W. Physisorption of Gases, with Special Reference to the Evaluation of Surface Area and Pore Size Distribution (IUPAC Technical Report). *Pure Appl. Chem.* **2015**, *87* (9–10), 1051–1069. https://doi.org/10.1515/pac-2014-1117.

(53) Weigler, M.; Brodrecht, M.; Breitzke, H.; Dietrich, F.; Sattig, M.; Buntkowsky, G.; Vogel, M. 2 H NMR Studies on Water Dynamics in Functionalized Mesoporous Silica. *Zeitschrift für Phys. Chemie* **2018**, *232* (7–8), 1041–1058. https://doi.org/10.1515/zpch-2017-1034.

(54) Salis, A.; Pisano, M.; Monduzzi, M.; Solinas, V.; Sanjust, E. Laccase from Pleurotus Sajor-Caju

on Functionalised SBA-15 Mesoporous Silica: Immobilisation and Use for the Oxidation of Phenolic Compounds. *J. Mol. Catal. B Enzym.* **2009**, *58* (1–4), 175.

(55) Larkin, P. J. Introduction. In *Infrared and Raman Spectroscopy*; Larkin, P. J. B. T.-I. and R. S. (Second E., Ed.; Elsevier, 2018; pp 1–5. https://doi.org/10.1016/B978-0-12-804162-8.00001-X.

(56) Boyd, R.; Smith, G. NMR Spectroscopy. In *Polymer Dynamics and Relaxation*; Cambridge University Press: Cambridge, 2001; Vol. 14, pp 44–56. https://doi.org/10.1017/CBO9780511600319.005.

(57) Miller, A. H.; de Vasconcellos, A.; Fielding, A. J.; Nery, J. G. Nanozeolites as Support for Laccase Immobilization: Application to Mediated Glycerol Oxidation. *Appl. Catal. A Gen.* **2021**, *626* (July), 118361. https://doi.org/10.1016/j.apcata.2021.118361.

(58) Wang, Z.; Ren, D.; Jiang, S.; Yu, H.; Cheng, Y.; Zhang, S.; Zhang, X.; Chen, W. The Study of Laccase Immobilization Optimization and Stability Improvement on CTAB-KOH Modified Biochar. *BMC Biotechnol.* **2021**, *21* (1), 47. https://doi.org/10.1186/s12896-021-00709-3.

(59) Vera, M.; Fodor, C.; Garcia, Y.; Pereira, E.; Loos, K.; Rivas, B. L. Multienzymatic Immobilization of Laccases on Polymeric Microspheres: A Strategy to Expand the Maximum Catalytic Efficiency. *J. Appl. Polym. Sci.* **2020**, *137* (47), 49562. https://doi.org/10.1002/app.49562.

(60) dos Santos, K. P.; Rios, N. S.; Labus, K.; Gonçalves, L. R. B. Co-Immobilization of Lipase and Laccase on Agarose-Based Supports via Layer-by-Layer Strategy: Effect of Diffusional Limitations. *Biochem. Eng. J.* **2022**, *185* (July), 108533. https://doi.org/10.1016/j.bej.2022.108533.

(61) Attanasio, A.; Diano, N.; Grano, V.; Sicuranza, S.; Rossi, S.; Bencivenga, U.; Fraconte, L.; Di Martino, S.; Canciglia, P.; Mita, D. G. Nonisothermal Bioreactors in the Treatment of Vegetation Waters from Olive Oil: Laccase versus Syringic Acid as Bioremediation Model. *Biotechnol. Prog.* **2005**, *21* (3), 806–815. https://doi.org/10.1021/bp0495724.

(62) Zheng, F.; Cui, B.-K.; Wu, X.-J.; Meng, G.; Liu, H.-X.; Si, J. Immobilization of Laccase onto

Chitosan Beads to Enhance Its Capability to Degrade Synthetic Dyes. *Int. Biodeterior. Biodegradation* **2016**, *110* (4), 69–78. https://doi.org/10.1016/j.ibiod.2016.03.004.

(63) Hu, J.; Yuan, B.; Zhang, Y.; Guo, M. Immobilization of Laccase on Magnetic Silica Nanoparticles and Its Application in the Oxidation of Guaiacol, a Phenolic Lignin Model Compound. *RSC Adv.* **2015**, *5* (120), 99439–99447. https://doi.org/10.1039/c5ra14982g.

(64) Girelli, A. M.; Quattrocchi, L.; Scuto, F. R. Silica-Chitosan Hybrid Support for Laccase Immobilization. *J. Biotechnol.* **2020**, *318* (March), 45–50. https://doi.org/10.1016/j.jbiotec.2020.05.004.

(65) Velásquez-Hernández, M. D. J.; Ricco, R.; Carraro, F.; Limpoco, F. T.; Linares-Moreau, M.; Leitner, E.; Wiltsche, H.; Rattenberger, J.; Schröttner, H.; Frühwirt, P.; Stadler, E. M.; Gescheidt, G.; Amenitsch, H.; Doonan, C. J.; Falcaro, P. Degradation of ZIF-8 in Phosphate Buffered Saline Media. *CrystEngComm* **2019**, *21* (31), 4538–4544. https://doi.org/10.1039/c9ce00757a.

(66) Bůžek, D.; Adamec, S.; Lang, K.; Demel, J. Metal-Organic Frameworks: Vs. Buffers: Case Study of UiO-66 Stability. *Inorg. Chem. Front.* **2021**, *8* (3), 720–734. https://doi.org/10.1039/d0qi00973c.

(67) Hashem, T.; Valadez Sanchez, E. P.; Bogdanova, E.; Ugodchikova, A.; Mohamed, A.; Schwotzer, M.; Alkordi, M. H.; Wöll, C. Stability of Monolithic Mof Thin Films in Acidic and Alkaline Aqueous Media. *Membranes (Basel).* **2021**, *11* (3), 1–12. https://doi.org/10.3390/membranes11030207.

(68) Shortall, K.; Otero, F.; Bendl, S.; Soulimane, T.; Magner, E. Enzyme Immobilization on Metal Organic Frameworks: The Effect of Buffer on the Stability of the Support. *Langmuir* **2022**, *38* (44), 13382–13391. https://doi.org/10.1021/acs.langmuir.2c01630.

(69) Smeets, V.; Baaziz, W.; Ersen, O.; Gaigneaux, E. M.; Boissière, C.; Sanchez, C.; Debecker, D. P. Hollow Zeolite Microspheres as a Nest for Enzymes: A New Route to Hybrid Heterogeneous Catalysts. *Chem. Sci.* **2020**, *11* (4), 954–961. https://doi.org/10.1039/C9SC04615A.